# A Highly Directive Dipole Antenna Embedded in a Fabry–Pérot Type Cavity

T. Akalin, J. Danglot, O. Vanbésien, and D. Lippens

***Abstract*—We investigate the origin of the directivity of a dipole antenna embedded in a dielectric slab Fabry–Pérot cavity. It is shown that the focusing effect is due to the angular selection rules in the Bragg-type mirror and is directly correlated to the frequency selectivity of the cavity. For a 6 GHz resonant device, having a quality factor of 100, the aperture of the beam pattern ($E$-$H$ plane) is close to 12° in agreement with the arguments based on frequency and angular selectivities. Hence, this kind of cavity could be used in free-space based communication links.**

***Index Terms*—Dielectric Bragg mirror, Fabry–Pérot cavity, high directive antenna.**

## I. Introduction

WIRELESS communications with electromagnetic wave propagation in free space are in need of directive antennas. Various means can be implemented for increasing the directivity of antennas, notably the insertion of a back reflector or the fabrication of antenna arrays. Recently, the electromagnetic properties of periodic structures were revisited, following the rapid development of the so-called photonic band gap microstructures whose concepts can be extended to the microwave spectrum. In this context, the Limoges University group [1], [2] has proposed a number of ways to take advantage of rf photonic dielectric multilayered structures with recently the proposal of a one-dimensional (1-D) photonic band gap antenna. This research direction was also investigated by Ozbay *et al.* [3], [4] with the same underlying idea taking benefit of metallic structures. In our research group, we have also studied a metal/dielectric structure periodically loaded with active devices [5], which can open the possibility to smart devices notably for steerable antennas via tunable phase shifters, back reflectors, or tunable impedance surface [6]. In this paper, we address the problem of fabricating highly directive antennas owing to their insertion in a microcavity. For the basic radiating element, we chose a simple dipole which exhibits a quasiisotropic radiation pattern when isolated. Also, one-dimensional Bragg mirrors without conformation define the electromagnetic cavity designed for operation in C-band. The concepts however can be easily scaled at higher frequencies, notably for indoor communication systems, with a proper technology. In Section II, we address the directivity and resonance issues on the basis of numerical electromagnetic simulations taking into account the finite dimensions of the Bragg mirrors. In Section III, we analyze the relationship between the frequency and angular selectivities via a quasi-one dimensional approach and we discuss the respective advantages of PBGs used as a mirror or as a lensing element.

Manuscript received June 1, 2001; revised November 13, 2001. The review of this letter was arranged by Associate Editor Dr. Ruediger Vahldieck.

The authors are with the Institut d'Electronique et de Microélectronique du Nord, Université de Lille, Cedex, France (e-mail: tahsin.akalin@IEMN.univ-lille1.fr).

Publisher Item Identifier S 1531-1309(02)01818-4.

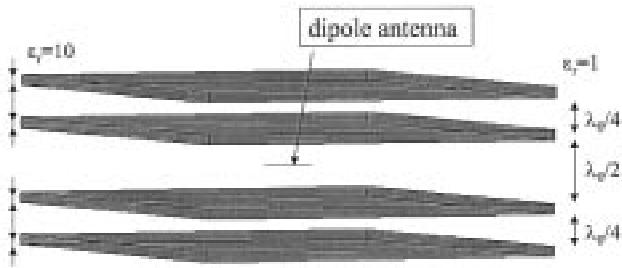


Fig. 1. Schematic of the dipole antenna embedded in a cavity bounded by Bragg mirror. The thicknesses are 3.96 mm for the dielectric plates and 12.5 mm for the air slabs.

## II. Numerical Results

A schematic diagram of the electromagnetic cavity used in the present work is given in Fig. 1. The cavity is bounded by two Bragg mirrors composed of alternating layers of a material with a high dielectric constant ($\varepsilon_r = 10$), such as the Duroid 6010 manufactured by Rogers, and air. For the present study, we chose a 6 GHz frequency of operation. Under these conditions, the characteristic dimensions of the Bragg mirrors are 3.96 mm for the dielectric layers spaced by 12.5 mm of air slabs. These dimensions yield a maximum reflectivity centered at 6 GHz with a reflectivity plateau (3 dB bandwidth) of 5.8 GHz.

The cavity is formed by suppressing one dielectric layer in the center of the structure corresponding to a $\lambda_0/2$ resonance condition at the frequency of interest.

Figure 2 shows the frequency dependence of the reflection coefficient calculated by means of electromagnetic simulations using HFSS code by Agilent. For the present study, the radiating element was set in the center of the cavity with square-shaped dielectric plates of 150 mm of side. Two minima are apparent in this figure at 6.16 GHz and 6.62 GHz, respectively. The corresponding radiation patterns are plotted in Fig. 3. For the first resonance, a high directive beam is thus demonstrated by a beam-width angle of 13°.

In order to have further insight into the confinement properties of the electromagnetic energy, Fig. 4 shows a pattern of the electric field in a cross section corresponding to the dipole location. For the high directive beam case (6.16 GHz), the field

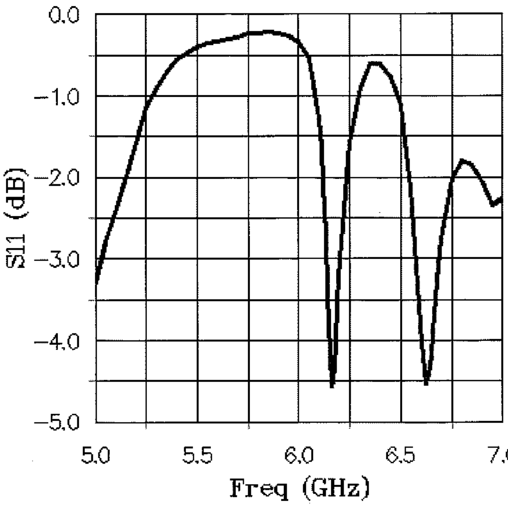


Fig. 2. Reflection coefficient versus frequency for 150 mm-side dielectric plates.

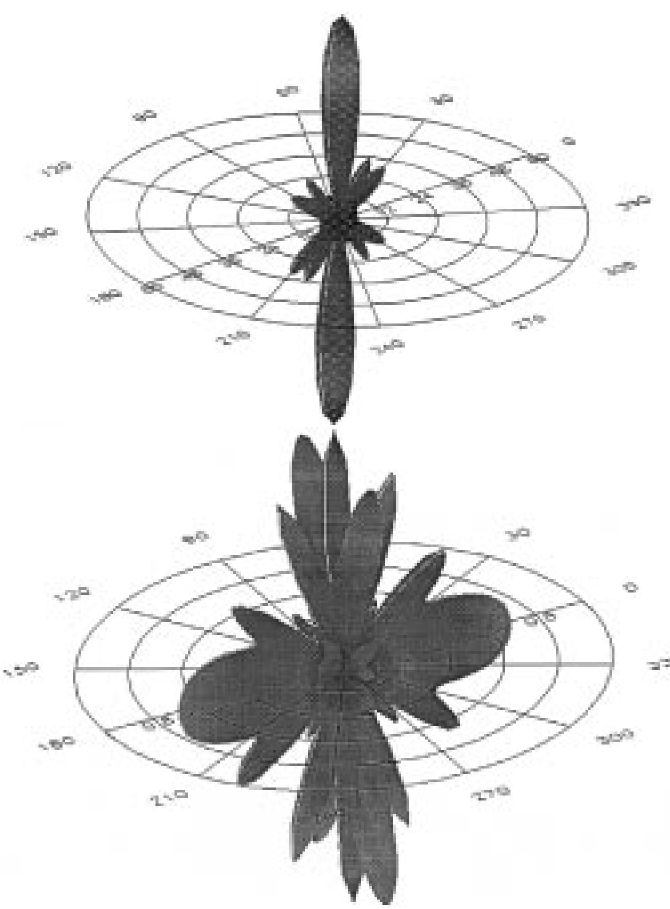

Fig. 3. Comparison between the radiation pattern of a dipole antenna with frequency corresponding to the first and second peaks in the reflection coefficient.

is well distributed within the cavity whereas side accumulation regions can be seen for the 6.62 GHz resonance.

## III. Directivity Analysis

At this stage, two issues can be discussed on the basis of the transmission properties of the empty cavity in order to highlight the frequency selectivity, whereas the evanescence properties of Bragg mirrors will explain why a high directivity is achieved. Fig. 5 is a plot of the transmission spectrum of a nonloaded cavity with infinite dielectric plates. A stop band resulting from the periodic arrangement of dielectric/air slabs extends from 3 GHz to about 9 GHz. If we model the devices as a one-dimensional (1-D) photonic crystal structure we can simulate the corresponding band gap. Following this approach, the sharp transmission peak at 6 GHz can be explained as a defect-assisted transmission effect. Provided the structure is symmetrical, a unitary transmission is obtained at the resonant frequency. This argument is still valid for an EM excitation within the cavity. This resonant effect explains why the double mirror device exhibits a high transmissivity whereas each mirror, taken separately, exhibits a high reflectivity (poor transmission). The same conclusions apply for electronic cavities [7] with a unitary transmission for double barrier microstructures where a resonant tunneling effect can be seen.

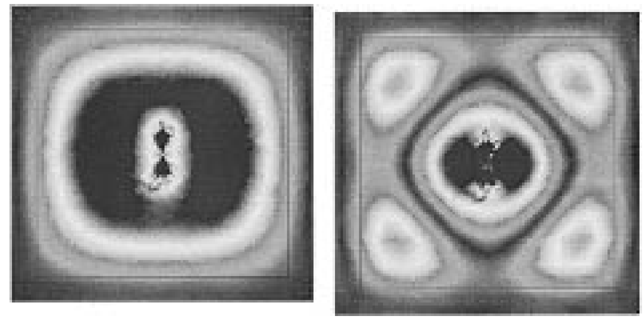

(a) (b)

Fig. 4. Illustration of the cavity modes with an electric field pattern in the dipole cross section (a) 6.16 GHz resonance (b) 6.62 GHz resonance. The darkest zones in the square delimited region correspond to the highest field strengths.

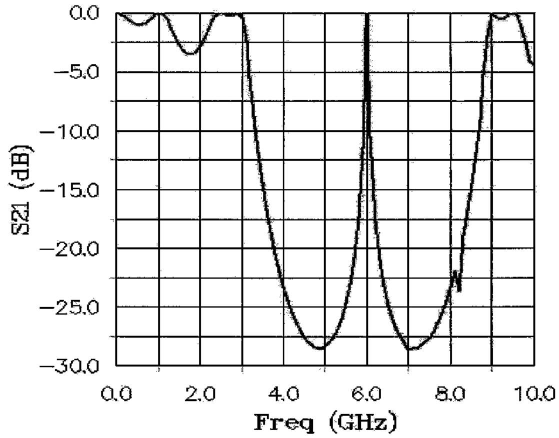


Fig. 5. Transmission coefficient through the empty cavity with infinite dielectric plates.

With respect to the directivity, we can further take advantage of the analogy between photonic and electronic devices by comparing the tunneling and evanescence properties within the confinement barrier (electronic device) or mirror (photonic component). It is now well known that the quantum transmission through a barrier can be described by the Wentzel-Kramers-Brillouin (WKB) approximation with a tunneling probability di-

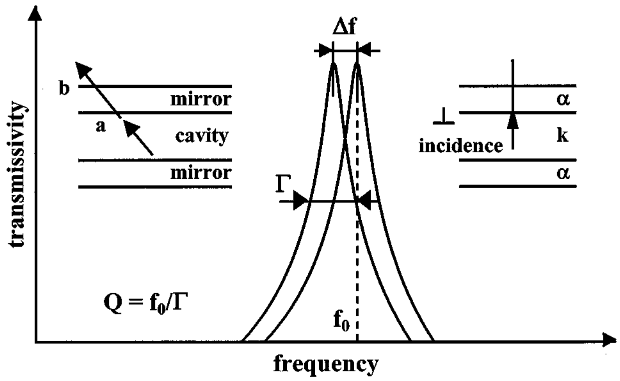


Fig. 6. Illustration of the analysis of the frequency and angular selectivities.

rectly related to the so-called turning points (locations where the $k$ vector becomes imaginary). Therefore, the quantum transmission probability $(P)$ along the $z$ axis is a decreasing exponential function of the integral of the attenuation factor $(\alpha)$ with a integration interval defined by the turning points $(P \sim \exp(-2\int \alpha\, dz)$. Under these conditions, the highest transmission level is achieved for a direction normal to the dielectric plate for which the difference between the turning points is minimum.

The close analogy between the solid state physics of semiconductors and photonic crystals [8] can also be used in order to analyze the relationship between the frequency and angular selectivities. To this aim, a quasi-1-D confinement condition can be assumed with infinite dielectric plates bearing in mind that additional confinement, as seen by numerical simulation can bring some corrections on the resonance conditions.

Fig. 6 illustrates the approach we have used by showing the transmission spectrum under resonant condition for a typical photonic or electronic cavity with a real $k$ vector within the cavity and an imaginary part in the confinement walls namely the Bragg mirrors for the photonic case. Under normal incidence the resonant frequency (energy) is $f_0$ with a full width at half maximum noted $\Gamma$. For a tilted situation, which is illustrated, on the left-hand side in Fig. 6, a shift in the resonant frequency can be expected depending on the tilt angle. The loss of transmissivity of the whole structure is a direct consequence of this shift. In other words, the frequency selectivity, quantified by the $Q$ factor $f_0/\Gamma$, also reflects the angular selectivity. In fact, the more the resonant process is frequency selective with a high quality factor of the photonic cavity the higher is the focusing effect by the insertion of the radiating element within the cavity. The exact relationship between the $Q$ factor and the typical angle where a transmissivity 3 dB lower is achieved will depend on the dispersion relation $E(k)$ or $\omega(\beta)$ which is quadratic for semiconductor and linear for photonic based structures. Simple algebra, using the quasi-1-D model, gives the following equation for $\theta_{\max}$ of photonic devices which can serve as a figure of merit for the directivity of the antenna:

$$\theta_{\max} = 2\,\mathrm{Arccos}(1 - 1/2Q). \tag{1}$$

In the case of small angles

$$\theta_{\max} = 2Q^{-1/2}. \tag{2}$$

Using $Q = 100$ for the empty cavity (Fig. 5), one finds $\theta_{\max} \sim 11.5°$. This value is the minimum intrinsic beam width which can be achieved for the proposed structure. Taking the finite dimensions of the dielectric slabs into account, we numerically found 13° in Section II. From (3), we can deduce inversely a quality factor close to 75 instead of 100 in a pure 1-D situation. This permits one to appreciate the impact of the two-dimensional (2-D) open character of the cavity.

For most applications, it is necessary to suppress one of the radiation direction, for instance, by means of a back-side metallic plate. Such a solution was demonstrated experimentally in [2] using a patch antenna. The dipole antenna used in the present work being less directive intrinsically (without an embedding cavity), it is believed that the focusing effect shown experimentally for a patch is also valid for a dipole which is initially a less favorable situation.

## IV. Conclusion

High directivity (about 12° for the beam width) can be achieved for antenna dipole embedded in a high quality factor (about 100) Fabry–Pérot cavity bounded by 1-D Bragg mirrors. The directivity was demonstrated numerically taking the finite dimension of the mirrors into account. The analysis of the angular selectivity was conducted through evanescence and resonant conditions. An inverse square root dependence was also estimated between the frequency and angular selectivities.

## Acknowledgment

This work was carried in the framework of the research group photonic crystal and microcavities of Centre National de la Recherche Scientifique (CNRS).

## References

[1] M. Thévenot, C. Cheype, A. Reneix, and B. Jecko, "Directive photonic band gap antennas," *IEEE Trans. Microwave Theory Tech.*, vol. 47, p. 2115, Nov. 1999.

[2] C. Serier, C. Cheype, R. Chantelat, M. Thévenot, T. Monédière, A. Reneix, and B. Jecko, "1-D photonic bandgap resonator antenna," *Microwave Opt. Technol. Lett.*, vol. 29, pp. 312–315, 2001.

[3] B. Temelkuran, E. Ozbay, J. P. Kavanaugh, G. Tuttle, and K. M. Ho, "Resonant cavity enhanced detectors embedded in photonic crystals," *Appl. Phys. Lett.*, vol. 72, p. 2376, 1998.

[4] E. Ozbay, B. Temelkuran, M. Sigalas, G. Tuttle, C. M. Soukoulis, and K. M. Ho, "Defect structures in metallic photonic crystals," *Appl. Phys. Lett.*, vol. 69, p. 3797, 1996.

[5] J. Danglot, O. Vanbésien, and D. Lippens, "Active waveguides patterned in a 2D-3D metallic photonic crystal," *Electron. Lett.*, vol. 53, p. 475, 1999.

[6] D. Sievenpiper, J. Schaffner, R. Loo, G. Tangonan, S. Ontiveros, and R. Harold, "Microwave beam steering reflector based on a tunable impedance surface," in *Proc. 30th EuMC Conf.*, Paris, Sept. 2000, p. 101.

[7] F. Podevin, O. Vanbésien, and D. Lippens, "Quantum calculations of conduction properties of metal/InAlAs/InGaAs heterostructures," *J. Appl. Phys.*, vol. 89, p. 6247, 2001.

[8] T. Akalin, J. Danglot, O. Vanbésien, and D. Lippens, "Highly directive antennas from $n$-dimensional photonic band, gap microcavities," presented at the *Proc. 24th ESTEC Antenna Workshop on Innovative Periodic Structure, Photonic Band Gap, Fractals, and Frequency Selective Surfaces*, Noordwijk, The Netherlands, May/June 2001.